Proceedings of ICRC 2001: 659 © Copernicus Gesellschaft 2001

ICRC 2001

A profile of EHE gamma-ray shower and its detection by the Telescope Array

N. Inoue[1], K. Shinozaki[1], H. P. Vankov[2], and M. Zha[3,4]

[1]Department of Physics, Saitama University, Saitama, Saitama, Japan
[2]Institute for Nuclear Research and Nuclear Energy, Sofia, Bulgaria
[3]Institute for Cosmic Ray Research, University of Tokyo, Kashiwa, Chiba, Japan
[4]Laboratory of Cosmic Ray and High Energy Astrophysics, Institute of High Energy Physics, Academia Sinica, Beijing 100039, China

Abstract. The nature and origin of Extremely High Energy(EHE) cosmic rays remains one of the great mysteries in modern astrophysics. One of the important tasks in Telescope Array project is an examination of chemical composition at energies greater than 10^{19}eV from a study of longitudinal developments of air showers. Characteristics of shower developments initiated by EHE gamma-ray primaries strongly depend on primary energy and arrival direction in comparison with ones of hadronic primaries.

1 Introduction

The primary composition of EHE cosmic rays has been studied by the experiments of Fly's Eye, Yakutsk and AGASA. However, it is still one of unsolved problems in high energy particle astrophysics.

Various models of the highest energy cosmic ray origin have been proposed (Rachen, 1993, Berezinsky, 1997 and Bhattacharjee, 1992).

In case of gamma-ray primaries, an influence of the Landau-Pomeranchuk-Migdal (LPM) effect (Landau, 1953 and Migdal,1956) on shower development has been studied and applied for simulation works by many authors. In general, this effect is an important mechanism to bremmsstrahlung and pair creation processes at extremely high energies to make characterize the gamma-ray shower development.

The other effect is a cascading in the geomagnetic field. A history of these calculations is long enough too and it started with the work by McBreen and Lambert,1981. Recent calculations (Stanev,1997) refined the previous ones revealing some practically important features in the cascading process.

Correspondence to: M. Inoue
(ninoue@post.saitama-u.ac.jp)

2 Simulation of EHE Gamma-ray Shower

To study on features of air shower developments initiated by EHE gamma-rays and hadrons (proton or iron) the AIRES simulation code(Ver.2.2.1;Sciutto, 1999) with QGSJET hadronic interaction model has been used in this work. In addition we made out our own code for electromagnetic cascading in the geomagnetic field. To simulate showers initiated by EHE gamma-rays, first we modeled cascading in the geomagnetic field starting with a single EHE gamma-ray far away from the Earth's surface down to the top of the atmosphere and connected to shower generated by AIRES.

It is well known that the essentially non-zero probabilities for magnetic bremsstrahlung and pair production are required in cases of strong geomagnetic field or high energy primary gamma-ray (Erber,1966). The relevant parameter determining the criteria for this is:

$$\chi = \frac{\varepsilon}{mc^2}\frac{H}{H_{cr}}$$

where ε is the particle energy, H is the magnetic field strength (the component normal to the particle trajectory), m is the electron mass and $H_{cr} = 4.41 \times 10^{13}$ G.

We used the differential probabilities (per unit length) for magnetic bremsstrahlung and magnetic pair production given by the expressions (Bayer,1973):

$$\pi(\varepsilon,\omega)\,d\omega = \frac{\alpha m^2}{\pi\sqrt{3}}\frac{d\omega}{\varepsilon^2}\times \left[\left(\frac{\varepsilon-\omega}{\varepsilon}+\frac{\varepsilon}{\varepsilon-\omega}\right)K_{\frac{2}{3}}\left(\frac{2u}{3\chi}\right)-\int\limits_{\frac{2u}{3\chi}}^{\infty}K_{\frac{1}{3}}(y)\,dy\right] \quad (1)$$

$$\gamma(\omega,\varepsilon)\,d\varepsilon = \frac{\alpha m^2}{\pi\sqrt{3}}\frac{d\varepsilon}{\omega^2}\times \left[\left(\frac{\omega-\varepsilon}{\varepsilon}+\frac{\varepsilon}{\omega-\varepsilon}\right)K_{\frac{2}{3}}\left(\frac{2u_1}{3\chi}\right)+\int\limits_{\frac{2u_1}{3\chi}}^{\infty}K_{\frac{1}{3}}(y)\,dy\right] \quad (2)$$

where ε and ω are the electron and photon energies and $u = \frac{\omega}{\varepsilon - \omega}$, $u_1 = \frac{\omega^2}{\varepsilon(\omega - \varepsilon)}$. Here $\hbar = c = 1$.

$K_\nu(z) = \int_0^\infty e^{-zch(t)} \mathrm{ch}(\nu t)\, dt$ is a modified Bessel function known as MacDonald's function.

While for $\chi \gg 1$ (strong field) the electromagnetic cascade develops similarly to the cascade in matter, in the region of $\chi \leq 1$ (geomagnetic field) the gamma-ray interaction length increases sharply with decrease of gamma-ray energy. Electrons continue to radiate and the shower becomes a bunch of secondary gamma-rays carrying $\geq 94 - 95\%$ of the primary energy.

In our simulation we used the International Geomagnetic Reference Field (IGRF) and World Magnetic Model (WMM) which provides a good approximation of the geomagnetic field up to 600 km from the ground and its extrapolation above this altitude. In this paper the properties of EHE gamma-ray showers are examined for the location of Utah, USA (133.0^oW, 39.5^oN and 1500m a.s.l.) .

We simulated the electromagnetic cascading by injecting EHE gamma-ray at a distance of 3 Earth's radii from the surface of the Earth. Primary gamma-ray and secondary particles were propagated with pair production and radiation taken into account on each step(a step-size of 1km). Only particles above the threshold energy of 10^{15}eV were followed in the simulation until they reach the top of the atmosphere.

Interaction probabilities of incident gamma-rays with the geomagnetic field have been estimated for different zenith and azimuthal angles of the arrival direction. Maps of average multiplicity of secondary particles at the top of atmosphere are shown for 4 different primary energies in horizontal coordinates in Fig.1. Multiplicity is related to an integration of magnetic field component perpendicular to a trajectory of cascading even if primary energy is fixed. The region with a smaller multiplicity is centered at 29^o in a zenith angle and a direction of 14^o west from the south which corresponds to the inverse direction of geomagnetic field. Its size shrinks quickly with an increase of primary energy. Fig.2 shows energy weighted spectra of secondary particles in geomagnetic cascading at the top of atmosphere for primary gamma-ray energies of $10^{19.5}$, $10^{20.0}$, $10^{20.5}$ and $10^{21.0}$eV drawn in each frame. Zenith angles are sampled as $39.7°$, $54.0°$ and $61.6°$ and azimuthal angles are assumed as north and south. Features of energy weighted spectra strongly depend on the arrival directions and primary energy. Primary gamma-rays without interaction to geomagnetic field can be found at the right end of energy weighted spectra in specific cases.

Successive shower developments in the atmosphere are constructed as a superposition of sub-showers initiated by secondary particles represented in energy spectra.

First library of sub-showers initiated by gamma-rays with energy between 10^{16}eV and 10^{21}eV was prepared by AIRES. Primary energies of gamma-rays are assigned with a log step of 0.1 over an energy range and 500 showers have been simulated for each entry. The number of electrons and all charged

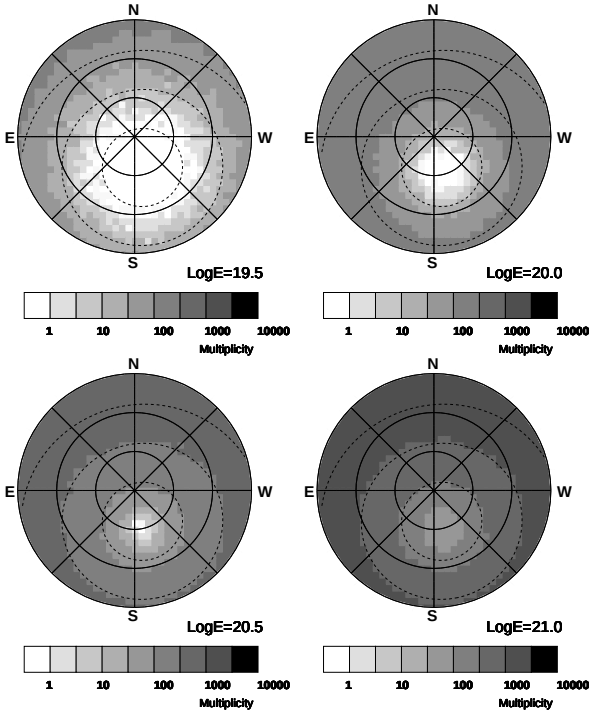

Fig. 1. Maps of average multiplicity of secondary particles (E$\geq 10^{15}$eV) at the top of atmosphere for primary gamma-ray energies of $10^{19.5}$eV, 10^{20}eV, $10^{20.5}$eV, and 10^{21}eV. Inner Circles show zenith angles of 30° and 60° and horizon. Dashed lines correspond to the angular distances of 30°, 60° and 90 ° to the inverse direction of geomagentic field at Utah.

particles for each shower was recorded at every 5 g/cm^2 step in vertical depth.

Simulations for proton and iron initiated air showers have been executed with the same primary energy interval. 500 showers for each entry have been simulated as the library set.

3 Results and Discussion

Fig.3 shows average X_{max}(an atmospheric depth at the shower maximum:$\langle X_{max} \rangle$) as a function of primary energy. $\langle X_{max} \rangle$s of gamma-ray primaries have been obtained for zenith angles of 54.0^o and 61.6^o(a broken and a solid line,respectively) and cases of south/north arrival directions are drawn in the figure. Ones of proton and iron primaries are also plotted with a solid and a dotted line in the same figure. While $\langle X_{max} \rangle$s of proton and iron showers are increasing with constant elongation rates of $54.2 gcm^{-2}$ and $56.0 gcm^{-2}$, ones of gamma-ray showers give a larger values with also invariable elongation rate up to $\sim 2 \times 10^{19}$eV. An elongation rate in higher energy region becomes larger with increasing gamma-ray energy as shown by open circles if the geomagnetic cascading process is not applied. The geomagnetic cascading starts its contribution to shower development above several

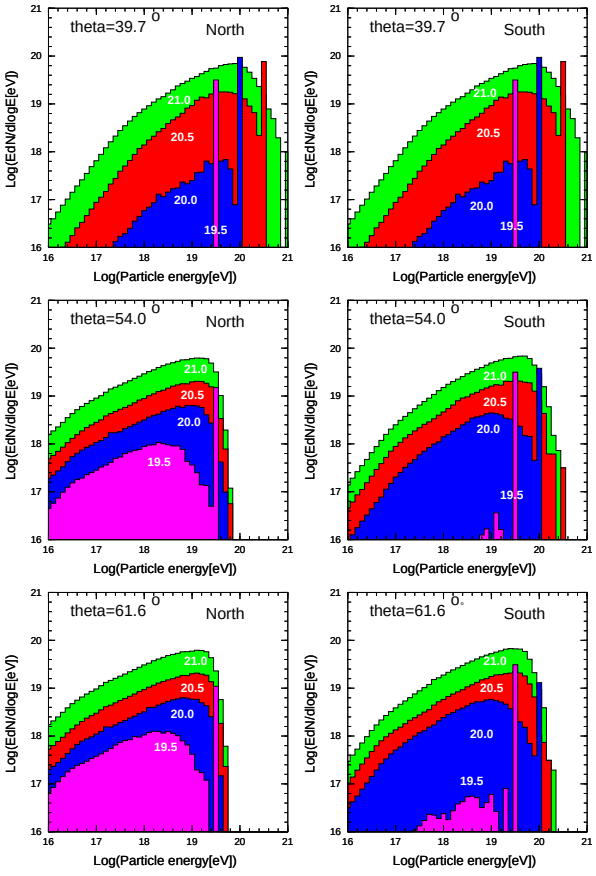

Fig. 2. Energy weighted spectra of secondary particles at the top of atmosphere for primary gamma-ray energies of $10^{19.5}$eV, $10^{20.0}$eV, $10^{20.5}$eV and $10^{21.0}$eV with 3 different zenith angles($39.7°$, $54.0°$ and $61.6°$). Azimuthal angles of primary gamma-rays are assumed as north and south.

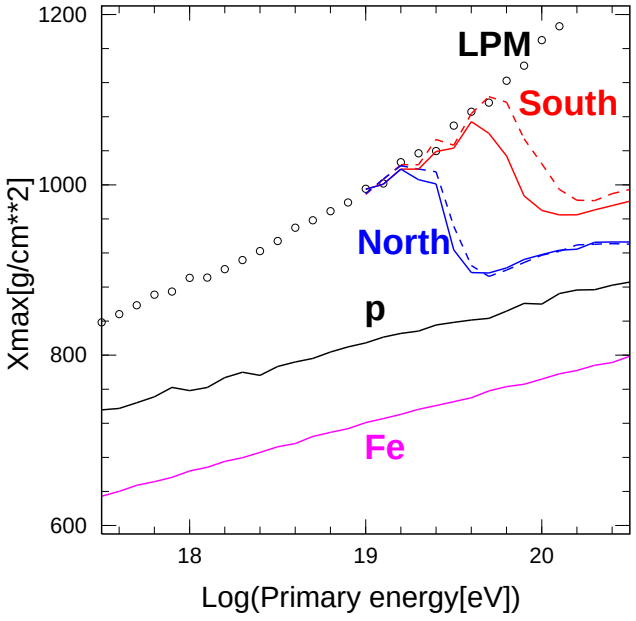

Fig. 3. Average X_{max} for showers initiated by protons, irons and gamma-rays as a function of primary energy. Proton and iron showers were simulated with AIRES-QGSJET. X_{max} of gamma-ray showers from south and north with zenith angles of $54.0°$(broken line) and $61.6°$(solid line) are shown.

times 10^{19}eV depending on the arrival direction of gamma-ray. Then, $\langle X_{max}\rangle$s decrease and reaches at the minimum. Shower development in atmosphere is almost equivalent to that of gamma-ray shower with a dominant energy of secondary component at the top of atmosphere. $\langle X_{max}\rangle$s increase again after the minima because an average energy of secondary particle becomes higher with increasing primary gamma-ray energy.

Fluctuations(standard deviation:σ) of X_{max} as a function of primary energy are shown for proton, iron and gamma-ray primaries in Fig.4. Results of proton and iron primaries are plotted by a broken and a dotted line, respectively. Zenith angles of 54.0^o and 61.6^o are assumed for gamma-ray primaries for each case of azimuthal directions of south and north as shown by open and closed circles. Though proton and iron showers have almost constant σ values as $67gcm^{-2}$ and $26gcm^{-2}$ over an energy range above 10^{18}eV, ones of gamma-rays have characteristic features depend on their primary energies. Dominant contribution of large fluctuation seen in an energy region between 19^{19}eV and 10^{20}eV is the influence of the mixed shower developments which are characterized with geomagnetic cascading on and off. Smaller fluctuation can be found in a higher energy region, as a result of shower developments which are constructed by a superposition of sub-showers initiated by secondary geomagnetic cascading particles. Fluctuation decreases quickly and reaches at the minimum within a change of primary energy less than $\Delta\log E_o$ of 0.5.

X_{max} distributions for showers initiated by protons and gamma-rays with energies of $10^{19.5}$, $10^{20.0}$ and $10^{20.5}$eV and zenith angles of 39.7^o, 54.0^o and 61.6^o are shown in Fig.5. An ambiguity of experimental determination in X_{max} is included as $30gcm^{-2}$ in these distributions. X_{max} distributions of gamma-rays also have not simple and change with primary energies and arrival directions because X_{max} of shower developments are affected by energy spectra of secondary particles in geomagnetic cascading. As seen in Fig.5, if primary gamma-rays interact with geomagnetic field and build up enough developed geomagnetic cascading, a smaller fluctuation of X_{max} is expected as σ of $\sim 60gcm^{-2}$, which is narrower than that of proton showers(σ of $\sim 110gcm^{-2}$) , which is typically seen in cases of showers coming from north with energies greater than 10^{20}eV. X_{max} distributions of gamma-rays coming from south have different features for any case of primary energies and arrival directions because they are composed of shower developments with rather weak or no contribution of geomagnetic cascading.

Telescope Array experiment is proposed to study on the origin and nature of EHE cosmic rays with a large statistics. The estimated annual event rates of cosmic rays are

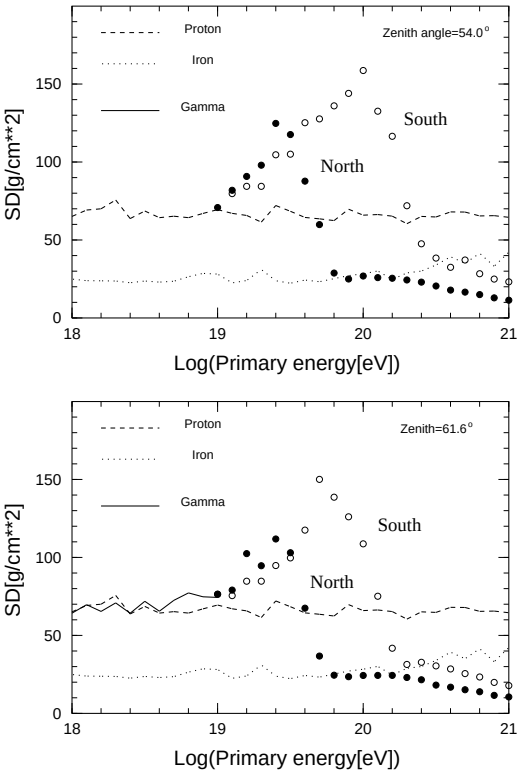

Fig. 4. Fluctuations(standard deviation:σ) of X_{max} as a function of primary energy. Proton, iron and gamma-ray primaries with zenith angles of 54.0^o and 61.6^o are assumed in the calculation. For gamma-ray primary fluctuations are drawn for cases of showers coming from south and north directions.

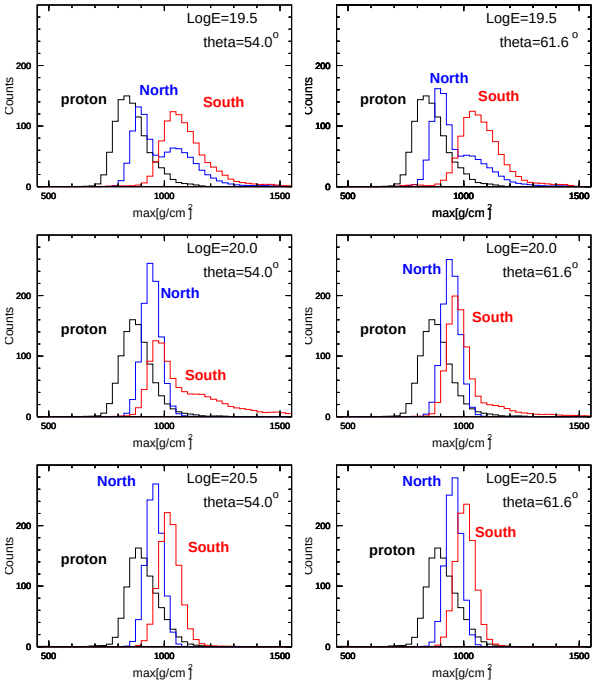

Fig. 5. X_{max} distributions for proton and gamma-ray showers with energies of $10^{19.5}$eV, 10^{20}eV and $10^{20.5}$eV (top, middle and bottom, respectively). Zenith angles of 54.0^o and 61.6^o (left and right) are assumed. X_{max} distributions of gamma-ray showers with arrival directions of south and north are shown in each figure. An ambiguity of experimental determination in X_{max} is included as $30gcm^{-2}$ in these distributions.

2000, 350 and 70 for energy regions of 10^{19}eV – 3×10^{19}eV, 3×10^{19}eV – 10^{20}eV and $>10^{20}$eV, respectively. The detection possibility of characteristic features contributed from gamma-rays as one of assumed primary compositions, depends on total statistics of expected cosmic rays and assumed gamma-ray flux in an overall energy spectrum. As seen in Fig.3, $\langle X_{max}\rangle$ of gamma-ray initiated showers is larger than that expected from proton initiated showers in an energy region less than 10^{19}eV. Furthermore, the elongation rates of gamma-ray showers show significant changes at different energies depending on their arrival directions. These properties of $\langle X_{max}\rangle$ in relation to primary energy and arrival direction are a possible key to study the gamma-ray flux through the observation of X_{max} with smaller statistical mean errors expected in an energy region between 10^{19} and 10^{20}eV. Also, behaviors of X_{max} fluctuations should be taking into account as one of parameters to characterize the feature as an additional information to $\langle X_{max}\rangle$ as seen in Fig.4. A study in an energy region greater than 10^{20}eV may need more elaborate considerations to acquire a definite conclusion because of insufficient statistics and smaller difference of shower developments between gamma-ray and proton primaries. A study on profiles of individual shower developments which will be measured at the best accuracy by Telescope Array at the highest energy region, will be preferable to discuss in paying an attention to their arrival directions as the first step. A quantitative estimations with the statistical significance for expected features included the contribution of gamma-ray showers have to treat carefully because they depend on nuclear interaction models in simulation and experimental uncertainties to determine X_{max} and primary energy for gamma-ray showers. Further progress in simulation study has to be desirable.

References

Bayer,V.H., Katkov,B.M. and Fadin,V.S., *,1973, Radiation of relativistic electrons(Moscow:Atomizdat)*

Berezinsky,V.,Kachelriess,M. and Vilenkin,A. *,1997, Phys. Rev. Lett.*, **79**, 4302

Bhattacharjee,P.,Hill,C.T. and Schramm,D.N. *,1992, Phys. Rev. Lett.*, **69**, 567

Erber,T., *,1966, Rev. Mod. Phys*. **38** 626

Landau,L.D. and Pomeranchuk,I.J. *,1953, Dokl. Akad. Nauk. SSSR*, **92**, 535

McBreen,B. and Lambert,C.J. *,1981, Phys. Rev. D*, **24**, 2536

Migdal,A.B. *,1956, Phys. Rev.*, **103**, 1811

Rachen,J.P. and Biermann,P.L., *1993, Astrophys.*, **272**, 161

Stanev,T. and Vankov,H.P. *,1997, Phys. Rev. D*, **55**, 1365

Sciutto,S.J. *,1999, GAP99-044*, AUGER technical note